

Anomalous Corrugations in Scanning Tunneling Microscopy: Imaging of Individual States

J. Tersoff

IBM Thomas J. Watson Research Center, Yorktown Heights, New York 10598

(Received 24 January 1986)

Unusual corrugations observed in scanning-tunneling-microscope (STM) images of 1T-TaS₂, Si(111)(2×1), and graphite are explained, and are shown to be characteristic of materials where the Fermi surface has collapsed to a point at the corner of the surface Brillouin zone. This is the first clear case where the low-bias STM image is dominated by electronic structure effects rather than surface geometry. Implications for STM spatial resolution are discussed.

PACS numbers: 61.16.Di

Scanning tunneling microscopy (STM) has proven uniquely useful because it gives direct real-space images of surfaces.¹ While electronic effects are sometimes detected, STM images are generally dominated by surface structural features. However, recently several cases have been found where experimental STM images exhibit unexpected large corrugations, which are not characteristic of the surface atomic geometry, and cannot be understood in purely structural terms.^{2–6}

This paper shows that these cases, 1T-TaS₂, Si(111)(2×1), and graphite, can be understood in terms of a single simple mechanism peculiar to semiconductors and semimetals of low effective dimensionality: Whenever the Fermi surface collapses to a point at the corner of the surface Brillouin zone (SBZ), the STM image corresponds in effect to an *individual state*. The nodal structure of this state gives rise to a large corrugation with the periodicity of the unit cell, regardless of the underlying atomic structure.

The theory⁷ of STM has already been applied very successfully in the usual case where atomic structure dominates the image.^{7,8} Attention has therefore turned to the effects of electronic structure in STM. Such effects may be enhanced to a dramatic extent by studying the dependence of the image on bias voltage,^{3,8} or by plotting differential tunneling conductance at a given bias voltage,^{9,10} and a theoretical investigation of such “scanning tunneling spectroscopy” has been reported by Selloni *et al.*¹¹

The first observation of dramatic electronic structure effects in ordinary STM, i.e., *without* voltage modulation or bias, was reported by Coleman *et al.*,² who imaged charge-density waves (CDW’s) on 1T-TaS₂. Surprisingly, very large corrugations (estimated 4 Å) with the CDW periodicity were observed, although the CDW atomic distortions are minute. No hint of the underlying atomic structure was observed. Subsequently several groups^{3–5} reported images of graphite with exceedingly large corrugations of roughly 1 Å (or even more, as discussed below), consistent¹² with the corrugation 0.7–1.0 Å calculated by Selloni *et al.*¹¹ The explanation offered here for these images,

which differ drastically from the surface topography, appears to be directly confirmed by subsequent observations of Stroscio, Feenstra, and Fein⁶ for tunneling to quasi one-dimensional chains on Si(111)(2×1).

The general theory of STM at small bias voltage has been discussed by Tersoff and Hamann.⁷ Within a simple s-wave model for the tip (whose actual structure is not known, and may vary from measurement to measurement), they found that the tunneling conductance σ is just

$$\begin{aligned} \sigma &\propto \rho(\mathbf{r}_t, E_F), \\ \rho(\mathbf{r}, E) &= \sum_{\nu} |\psi_{\nu}(\mathbf{r})|^2 \delta(E_{\nu} - E), \end{aligned} \quad (1)$$

where $\rho(\mathbf{r}_t, E_F)$ is the local density of states of the bare surface at the center of curvature \mathbf{r}_t of the tip and at the Fermi energy E_F , and ψ_{ν} are eigenstates of the semi-infinite sample with energy E_{ν} . The STM image (in the usual constant-current mode¹) then represents simply a contour of constant $\rho(\mathbf{r}, E_F)$.

In the usual case where the Fermi surface is extended, the image (1) is often quite similar to the total charge density.⁷ The crucial point of this paper is that there are, however, cases where only *one* surface wave vector \mathbf{k}_{\parallel} (or at most a set of symmetry-related \mathbf{k}_{\parallel} and their neighborhoods) contributes to the sum in (1). One is then in effect *imaging a single wave function*, rather than mapping surface topography. If \mathbf{k}_{\parallel} lies at the SBZ edge, that wave function will generally have nodes, which lead to very large corrugations with the periodicity of the unit cell, *independent of the atomic positions* within the unit cell.

The physics underlying the anomalous corrugations is conveniently illustrated by considering the quasi one-dimensional free-electron system, which has plane-wave eigenstates of the form $\psi_k = \exp(ikx)$. Here x is the allowed direction of propagation, z is the surface normal, and structure in the y direction is neglected. Outside the sample, the decaying tails of the states have the generalized plane-wave form⁷

$$\psi_k = \exp(ikx) \exp(-\alpha_k z), \quad (2)$$

where z is the surface-normal direction, $\alpha_k = (\alpha_0^2 + k^2)^{1/2}$, $\alpha_0 = \hbar^{-1}(2m\phi)^{1/2}$, and ϕ is the (effective local) work function.

If the crystal potential has a Fourier component $2k_F$, it opens up a gap at E_F , mixing states of wave vector k_F and $-k_F$ to form standing waves with nodes. The potential may have this periodicity either because $2k_F$ is the reciprocal-lattice vector G of the lattice, as for common semiconductors, or because of a $2k_F$ CDW distortion. (In discussing semiconductors, tunneling to band-edge states is assumed here, except as discussed below.)

With the assumption of inversion symmetry, the eigenstates of the crystal at E_F are then $\psi_k \pm \psi_{-k}$, and one can without loss of generality consider only one sign. Then, by use of (2), outside the crystal the wave function becomes

$$\Psi_k = \sin(k_F x) \exp(-\alpha_F z), \quad (3)$$

and from (1) the associated tunneling conductance is

$$\sigma = A_0 \sin^2(k_F x_t) \exp(-2\alpha_F z_t). \quad (4)$$

Here x_t and z_t specify the tip position, α_F is α_k at k_F , and the proportionality constant A_0 depends upon the experimental and material parameters.

The experimental image is the path of constant conductance,¹ defined implicitly by (4). Solving for z_t gives an image which can be cast in the dimensionless form

$$\zeta = \zeta_0 + \ln \sin^2 \eta, \quad (5)$$

where $\zeta = 2\alpha_F z_t$, $\eta = k_F x_t$, and $\zeta_0 = -\ln(\sigma/A_0)$. This function is shown in Fig. 1 and gives the STM image, within the approximation (1), for any realization of the two-plane-wave model. Only the scale of the axes and the z position of the surface plane depend on the specific case.

This idealized image consists of an array of singular dips, and is only physically meaningful outside the surface, where (3) is valid. In reality these dips will be smoothed out by a variety of effects. Most important, the result (1) depended upon the specific assumption of an s -wave tip wave function. That result was shown not to be very sensitive to the inclusion of the other low- l components.⁷ However, the vanishing conductance for $x_t=0$ is exact only when the tip wave function has no components of azimuthal symmetry $m_z \neq 0$. Thus one might expect a small parallel conductance channel associated with these tiny neglected terms, which could reduce the pathology at $x_t=0$ to merely a huge dip.

Other possible deviations from the idealized situation assumed here include nonideal instrumental response, and tunneling to states with \mathbf{k}_{\parallel} slightly off the symmetry point (due to finite Fermi-surface extent or to finite voltage). In particular, if the \mathbf{k}_{\parallel} range

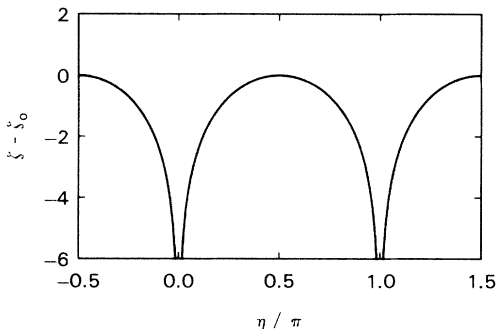


FIG. 1. Calculated STM image (5) for the two-plane-wave model of a one-dimensional semiconductor or CDW insulator.

sampled at voltage V , i.e., $k(E_F + eV) - k_F$, is a substantial fraction of the SBZ dimension, then the anomalous corrugation enhancement could be reduced or eliminated. Such an effect has apparently been observed in all the relevant systems studied experimentally,^{3,4,6,13} and is seen in the numerical calculation of Selloni *et al.*¹¹

The two-plane-wave approximation may seem simplistic. However, a crucial point here is that this model (or its 2D analog) is in fact quite adequate to describe the electronic structure at the distances of interest here. The real wave function, even if atomic-like, can be expanded in surface reciprocal-lattice vectors G as⁷

$$\Psi_k = \sum_G a_G \exp[i(k+G)x] \exp(-\alpha_G z), \quad (6)$$

where $\alpha_G = [\alpha_0^2 + (k+G)^2]^{1/2}$. (Any CDW's are assumed commensurate.) The higher Fourier components have larger α_G , and so decay faster with distance from the surface. At large enough distances, it is adequate, as in the two-plane-wave model, to retain only the two most slowly decaying terms. This is illustrated below for graphite. Thus the image in this case contains no information whatever on the positions of individual atoms.

The occurrence of this effect has subsequently been directly confirmed by Stroscio, Feenstra, and Fein,⁶ who observed an unexpected corrugation, with the periodicity of the lattice, along the quasi one-dimensional chains of Si(111)(2×1) when tunneling to surface states at the SBZ edge. These images had at first proven puzzling, because of their dissimilarity to the atomic structure. However, the phase change of the corrugation between valence-band and conduction-band images provided an unambiguous identification of the effect.

Real CDW materials are often quasi 2D, with a hexagonal structure consisting of three CDW's at 120° angles. Generalizing to quasi 2D materials is straightforward. If the band edge falls at \bar{P} , the relevant wave function can be expanded in six plane waves, and just

as in (5) the image can be cast in a dimensionless form:

$$\zeta = \ln \left(\sum_{n=1}^3 \sin^2 \hat{\omega}_n \cdot \eta \right) + \zeta_0, \quad (7)$$

where the CDW directions $\hat{\omega}_n$ are $(0,1)$, $(\frac{1}{2}\sqrt{3}, -\frac{1}{2})$, and $(-\frac{1}{2}\sqrt{3}, -\frac{1}{2})$. This model image exhibits a hexagonal array of singular dips. Along the shortest path between nodes, i.e., normal to $\hat{\omega}_1$, (7) is identical to the one-dimensional example above.

It seems probable that (7) is adequate to describe the image of a real CDW semiconductor such as $1T\text{-TaS}_2$, once allowance is made for smoothing as discussed above. This interpretation provides a natural explanation for the absence of observable CDW corrugation for the metallic $2H$ phase. However, the experimental images² do not show sufficient detail to provide a severe test, and *ab initio* calculations for such materials are not at present feasible. Fortunately the same physical effect is expected, and has apparently been observed,³⁻⁵ in a much simpler system, ordinary graphite.

Because of the weak interaction between layers in graphite, most electronic properties are already well described by a single monolayer,¹⁴ and so I consider that simplest system first. The graphite monolayer¹⁴ is a zero-gap semiconductor, with a single state at the corner \bar{P} of the SBZ determining E_F . This is exactly the situation described above for a hexagonal CDW, so that the (idealized) STM image of graphite should be well described by (7). At the same time, $\rho(\mathbf{r}, E_F)$ may be calculated directly, and the result of such a calculation is shown in Fig. 2, along with a schematic picture of the graphite structure and SBZ. The pi-state lobes directly over the atoms are clearly visible in Fig. 2, as is the node over the sixfold hollow site. The total charge density of the monolayer is also shown for comparison. The model image (7) is also shown in Fig. 2, and is virtually indistinguishable from the full calculation for graphite, except very near the surface where higher Fourier components of (6) cannot be neglected.

In real graphite, interlayer interactions yield a very narrow but finite Fermi surface, which lifts the strict node in $\rho(\mathbf{r}, E_F)$. These interactions also break the sixfold symmetry, making the two atoms inequivalent.^{3,11} It would be of some interest to see whether greatly expanding the Fermi surface by intercalation of alkali-metal atoms would drastically reduce the STM corrugation.

Note that the corrugation of the total charge density decays exponentially with distance from the surface.^{7,15} While normally this is true of the corrugation of $\rho(\mathbf{r}, E_F)$ as well,⁷ for this special case (7) shows explicitly that successive contours (within the six-plane-wave approximation) differ only by a constant shift in

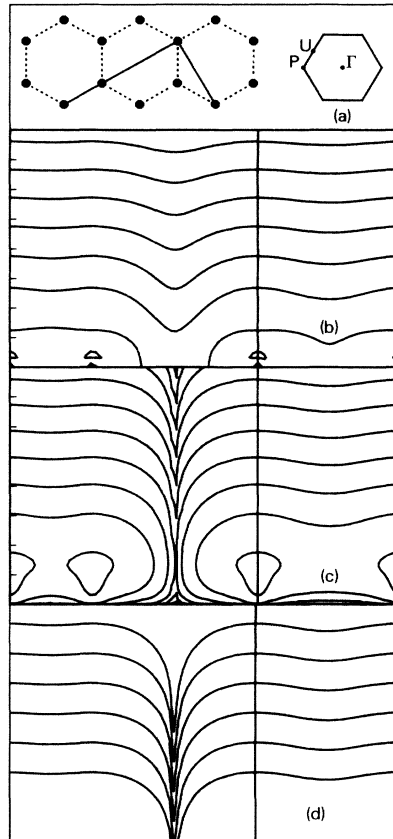


FIG. 2. (a) Surface Brillouin zone (SBZ) of hexagonal lattice (right), and structure of graphite monolayer. Circles: atoms; dotted lines: bonds; solid lines: planes of figures below. Horizontal and vertical axes are x and y . (b) Total charge density of graphite monolayer. Successive contours differ by a factor of ten. Ticks at left show intervals of 1 a.u. from surface (z direction). Atomic plane is at bottom. Horizontal axis corresponds to solid line in (a). (c) $\rho(\mathbf{r}, E_F)$ for graphite monolayer, as in (b). From (1), successive contours give possible STM images. (Details of singularity are truncated, a plotter artifact.) (d) Universal six-plane-wave model (7) of STM image for \mathbf{k}_F at \bar{P} in SBZ. Scale is chosen to correspond to graphite, and image is repeated with several displacements ζ_0 for ease of comparison.

the z direction.

The distance independence of the corrugation, as embodied in (7), has important implications for STM resolution. In particular, claims^{3,4} of extremely high resolution in STM based on the ability to image the unit cell in graphite, while correct, may possibly be misleading. While the resolution cannot be uniquely defined for a nonlinear measurement such as STM, in the large-distance (small corrugation) limit the problem can be linearized. Following Ref. 7, one can show that the effective resolution is then given by an rms

width W of

$$W(z_t) = \ln[\rho_G(z_t)\rho_G^{-1}(0)\rho_0^{-1}(z_t)\rho_0(0)]/2G^2,$$

where G is the smallest surface reciprocal-lattice vector, and ρ_0 and ρ_G are the zero and G Fourier components of $\rho(\mathbf{r}, E_F)$. When the assumption of sampling “typical” wave functions applies, W becomes rather insensitive to the sample details, and one can define an inherent resolution of the instrument⁷ $W(z_t) \approx (z_t/2\alpha)^{1/2}$, which broadens with increasing distance z_t . However, in the present case, it is simple to show that $\rho_G(z_t)\rho_G^{-1}(0) = \rho_0(z_t)\rho_0^{-1}(0)$, so that $W(z_t) \rightarrow 0$ independent of z_t , and the resolution so defined is infinite. Of course, for this case the asymptotic limit never applies, but the point remains that one expects remarkable resolution in the case of graphite which will not be reproducible on other surfaces, and so is not the characteristic resolution of the instrument.

For graphite, corrugation amplitudes of 3 Å or more have been observed, comparable to those for 1T-TaS₂. From (5) and (7), the corrugation amplitude scales with α_F , which is related to the work function as discussed under (2). Experimentally, measured values of $-d(\ln\sigma)/dz_t$, which should equal $2\alpha_F$, are instead usually much smaller, corresponding to an unphysically small “effective work function.” Comparison of theory and experiment¹⁶ suggests that, with suitable smoothing, (5) quantitatively describes experimental results for graphite, if the measured value of $-d(\ln\sigma)/dz_t$ is used for $2\alpha_F$. Unfortunately this quantity is not routinely measured during STM imaging. The small “effective work functions,” which should contribute to the large observed corrugations simply by distorting the z scale, are not well understood at this time, but explanations based on elastic deformations have been proposed by Coombs and Pethica¹⁷ and by Soler *et al.*¹⁸

In conclusion, for one- or two-dimensional semiconductors or semimetals, where the Fermi surface has collapsed to a point at the corner of the SBZ, the STM image is described in the ideal case by an extremely simple universal form. The crucial feature of this image is that it exhibits a large corrugation with the periodicity of the lattice, because of the nodal structure of the zone-edge wave function; the image has no direct relation to the positions of atoms within the unit cell. Moreover, while one can often neglect the sample dependence of the STM resolution,⁷ in the cases treated here the nominal resolution diverges because of the sample electronic structure, permitting easy resolution of 2-Å features on graphite.

It is a pleasure to thank P. K. Hansma for calling these intriguing systems to my attention, him and

N. Garcia for useful discussions, J. A. Stroscio, R. M. Feenstra, and A. P. Fein for permission to cite their results prior to publication, D. R. Hamann for the linearized-augmented-plane-wave code used to generate the graphite figures, and N. D. Lang and S. T. Pantelides for helpful comments.

¹G. Binnig, H. Rohrer, Ch. Gerber, and E. Weibel, Phys. Rev. Lett. **49**, 57 (1982); G. Binnig and H. Rohrer, Sci. Am. **253**, No. 2, 50 (1985).

²R. V. Coleman, B. Drake, P. K. Hansma, and G. Slough, Phys. Rev. Lett. **55**, 394 (1985); C. G. Slough, W. W. McNairy, R. V. Coleman, B. Drake, and P. K. Hansma, unpublished.

³G. Binnig, H. Fuchs, Ch. Gerber, H. Rohrer, E. Stoll, and E. Tosatti, Europhys. Lett. **1**, 31 (1986).

⁴S. Park and C. F. Quate, Appl. Phys. Lett. **48**, 112 (1986).

⁵P. K. Hansma, Bull. Am. Phys. Soc. **30**, 251 (1985).

⁶J. A. Stroscio, R. M. Feenstra, and A. P. Fein, to be published.

⁷J. Tersoff and D. R. Hamann, Phys. Rev. B **31**, 805 (1985), and Phys. Rev. Lett. **50**, 1998 (1983).

⁸R. M. Tromp, R. J. Hamers, and J. E. Demuth, Phys. Rev. B **34**, 1388 (1986).

⁹R. S. Becker, J. A. Golovchenko, D. R. Hamann, and B. S. Swartzentruber, Phys. Rev. Lett. **55**, 2032 (1985); R. J. Hamers, R. M. Tromp, and J. E. Demuth, Phys. Rev. Lett. **56**, 1972 (1986).

¹⁰G. Binnig, K. H. Frank, H. Fuchs, N. Garcia, B. Reihl, H. Rohrer, F. Salvan, and A. R. Williams, Phys. Rev. Lett. **55**, 991 (1985).

¹¹A. Selloni, P. Carnevali, E. Tossati, and C. D. Chen, Phys. Rev. B **31**, 2602 (1985).

¹²Reference 11 concerned voltage-dependent STM, and so used a general-purpose sampling of wave vector and energy, which should underestimate the corrugation for the strict zero-voltage limit unless the sampling is finer than the projected Fermi-surface dimensions (since numerically one otherwise never samples just the states at E_F and \bar{P}). The result of Ref. 11 therefore represents a lower bound on the corrugation of $\rho(\mathbf{r}, E_F)$.

¹³P. K. Hansma, private communication.

¹⁴G. S. Painter and D. E. Ellis, Phys. Rev. B **1**, 4747 (1970). The slight inequivalence of the two atoms in the surface unit cell, discussed in Ref. 11, is of course absent in the monolayer. For real (3D) graphite, see R. C. Tatar and S. Rabii, Phys. Rev. B **25**, 4126 (1985).

¹⁵J. Tersoff, M. J. Cardillo, and D. R. Hamann, Phys. Rev. B **32**, 5044 (1985).

¹⁶J. Schneir, R. Sonnenfeld, P. K. Hansma, and J. Tersoff, to be published.

¹⁷J. H. Coombs and J. B. Pethica, IBM J. Res. Dev., to be published.

¹⁸J. Soler, A. M. Baro, N. Garcia, and H. Rohrer, following Letter [Phys. Rev. Lett. **57**, 444 (1986)].